INTERNATIONAL JOURNAL FOR NUMERICAL AND ANALYTICAL METHODS IN GEOMECHANICS, VOL. 21, 277–291 (1997)

IDENTIFICATION OF DEFECTS IN PILES THROUGH DYNAMIC TESTING

SHUTAO T. LIAO* AND JOSE M. ROESSET†

*Department of Civil Engineering, Chung-Hua Polytechnic Institute, Hsin-Chu 30067, Taiwan
†Department of Civil Engineering, The University of Texas at Austin, Austin, TX 78712-1076, U.S.A.

SUMMARY

The objective of this work was to evaluate the theoretical capabilities of the non-destructive impact-response method in detecting the existence of a single defect in a pile, its location and its length. The cross-section of the pile is assumed to be circular and the defects are assumed to be axisymmetric in geometry. As mentioned in the companion paper, special codes utilizing one-dimensional (1-D) and three-dimensional (3-D) axisymmetric finite element models were developed to simulate the responses of defective piles to an impact load. Extensive parametric studies were then performed. In each study, the results from the direct use of time histories of displacements or velocities and the mechanical admittance (or mobility) function were compared in order to assess their capabilities. The effects of the length and the width of a defect were also investigated using these methods. © 1997 by John Wiley & Sons, Ltd. Int. j. numer. anal. methods geomech., vol. 21, 277–291 (1997)

(No. of Figures: 15 No. of Tables: 0 No. of Refs: 2)

Key words: defects in piles; dynamic testing; non-destructive impact-response method

1. INTRODUCTION

The existence of possible defects due to voids or inclusions in a pile after construction is always a main issue in the quality control of deep foundations. As a result there has been for years a strong interest in finding effective (fast and economical) non-destructive procedures to determine the length and cross-sectional area of an as-built, cast-in-place pile (or pier) and to identify and locate potential defects. This paper is the second part of a continuing work[1] aimed at exploring the capabilities of various techniques to determine the characteristics (length and cross-sectional area) of intact piles and to locate defects when these are present. The methods are evaluated by looking at the results of numerical analyses to assess the clarity and accuracy with which known parameters could be predicted. The models used and the numerical formulation were presented and discussed in the companion paper[1] devoted to the study of intact piles. In this paper the effects of existing defects on the time histories of the displacements and velocities that would be recorded theoretically at the top of the pile and on the mechanical admittance are investigated.

* Associate Professor
† Joe J. King Chair in Engineering

CCC 0363–9061/97/040277–15$17.50

Received 1 March 1996
Revised 20 August 1996

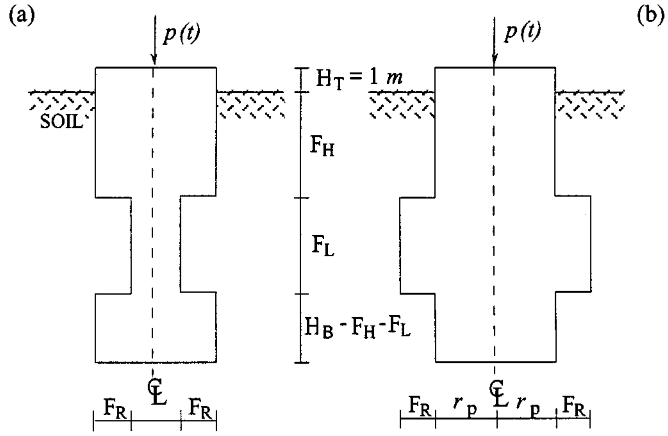

Figure 1. Geometric definition of (a) a neck and (b) a bulb

2. PROBLEM DEFINITION

2.1. Geometry

Consider the intact pile studied in the previous paper with a total length of $L = 12$ m. The pile has a circular cross-sectional area with a radius $r_P = 0{\cdot}5$ m. The lengths of the pile above and below ground are $H_T = 1$ and $H_B = 11$ m, respectively. As shown in Figures 1(a) and (b), an axisymmetric neck and bulb are introduced in the model of the pile as potential defects to assess the capability of the impact response (or impulse response) method to locate them. They are defined by the embedment depth F_H, the extension F_R in the radial direction from the lateral surface to the pile, and the length F_L. The applied loading $p(t)$ is a sinusoidal impact pressure of half a cycle duration with a period of $2T_d$ second where $T_d = 1{\cdot}5 \times 10^{-3}$ s. The peak pressure of this impact is 15, 570 N/m^2 and the radius of the loaded area is set at $r_L = 0{\cdot}0254$ m. In the 3-D finite element model, the receiver is placed 0·4 m away from the axis on the top surface of the pile.

The Young's modulus, mass density, and Poisson's ratio of the soil used for the study are $E_s = 1{\cdot}8 \times 10^8$ N/m^2, $\rho_s = 1924$ kg/m^2 and $v_s = 0{\cdot}4$. For the pile, which is assumed to be made of concrete, $E_c = 3{\cdot}31 \times 10^{10}$ N/m^2, $\rho_c = 2300$ kg/m^3 and $v_c = 0{\cdot}2$.

In using the 1-D model to simulate a pile with a defect, it must be taken into account that the radius of the pile is not constant through its whole length. The radius of the pile will decrease to $r_P - F_R$ in the case of a neck and increase to $r_P + F_R$ when dealing with a bulb, as shown in Figure 1. Therefore the pile is divided into elements with different radii. The values of the radius of each element affects not only the stiffness and mass per unit length of the pile but also the values of the dashpots along the pile and the bottom spring and dashpot.

3. RESULTS AND DISCUSSION

3.1. Effects of models

3.1.1. Neck. The defective pile with a neck shown in Figure 1(a) was considered first. The neck begins at $F_H = 5$ m with $F_R = 0{\cdot}2$ and $F_L = 1$ m. The displacement time histories obtained with

the 1-D and 3-D models are presented together in Figure 2(a). It can be seen that the results from these two models are very close to each other but the 3-D results can be dramatically reduced, as shown in Figure 2(b), when the components higher than a specific frequency $f_H = 500$ Hz are filtered out. The theoretical times of arrival of the longitudinal waves reflected from the neck and the bottom are marked in the figure with 'NECK' and 'BTM'. From these results it is concluded that a one-dimensional model can be satisfactorily used to predict the response. The 1-D solution is then compared with that of an intact pile in Figure 2(c). It can be seen that a neck results in another dip in the time record of the amplitude of the downward displacement. It is also seen that the theoretical times of arrival of the waves agree well with the occurrence of downward excursions in the curves as predicted by the finite element results.

The velocity time histories corresponding to the displacements shown in Figure 2 are presented in Figure 3 over the smaller time range $0 \leqslant t \leqslant 15 \times 10^{-3}$ which is the one of practical interest according to the displacement traces. From Figure 3(a) it is seen that identifying the times of

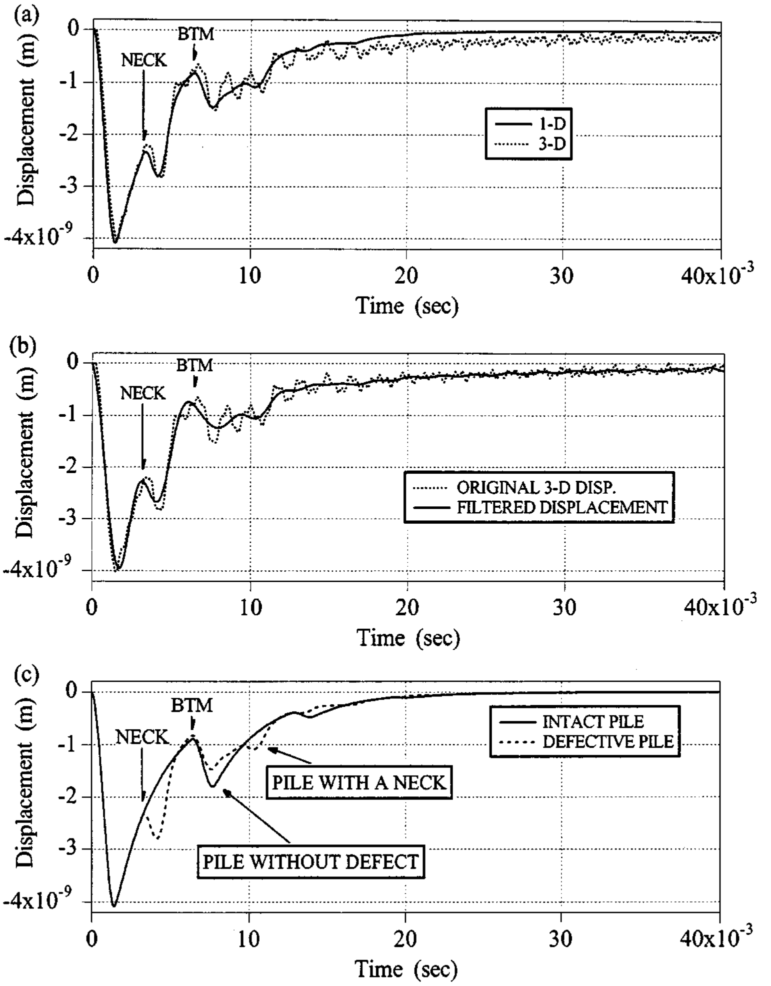

Figure 2. Displacement at top of a pile containing a neck with $F_H = 5$, $F_R = 0{\cdot}2$, and $F_L = 1$, using (a) 1-D and 3-D models, (b) 3-D filtered results ($f_H = 500$ Hz) and (c) 1-D results in comparisons with those of an intact pile

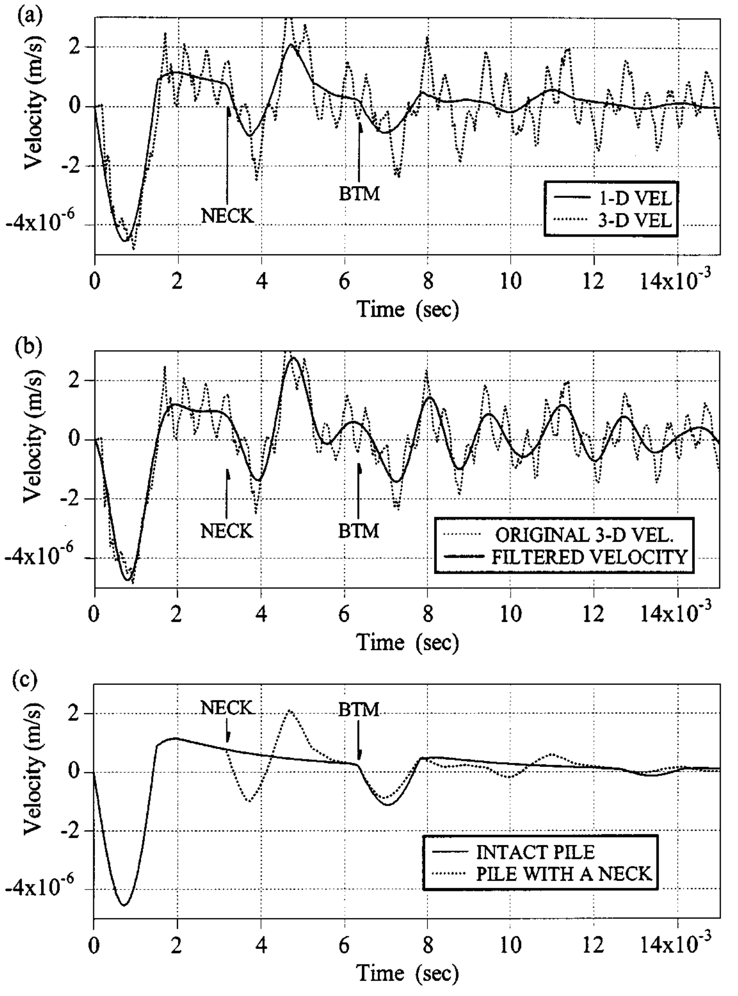

Figure 3. Velocity at top of a pile containing a neck with $F_H = 5$, $F_R = 0{\cdot}2$, and $F_L = 1$, using (a) 1-D and 3-D models, (b) original and filtered 3-D results ($f_H = 1000$ Hz) and (c) 1-D results in comparisons with those of an intact pile

arrival of the waves reflected from the neck and the bottom of the pile is straightforward in the velocity records, especially from the 1-D model. The identification of the arrivals of the reflection waves is more difficult for the 3-D results. The filtering technique was again used to clarify and smooth the results of the 3-D model. The velocity record from the 3-D model after filtering out the components corresponding to frequencies higher than 1000 Hz is presented in Figure 3(b). For the velocity records a higher threshold frequency can be used (1000 instead of 500 Hz) with excellent results. The use of 500 Hz provided very similar results. It is seen that the filtered solutions are much easier for evaluation work than the original 3-D results, which may be more representative of the data obtained from the *in situ* tests. This suggests that filters should be used in the collection of the experimental data, which is indeed done in practice. From the comparisons indicated in Figure 3(c) with the 1-D results for an intact and a defective pile (with a neck), it is clear that locating the neck from the early arrival of the reflected waves is rather straightforward in the case considered.

The mechanical admittance method can be alternatively used to analyse the response of the defective pile discussed above. The mechanical admittance curve of this pile is presented in Figure 4. To avoid the interference of the high-frequency fluctuations found in the results from the 3-D models, the results obtained with the 1-D models were used.

In locating a defect and determining its length from the mechanical admittance analysis, the most important principle is to find the periodicity implicit in the resulting curve. A periodicity in the curve may be defined by selecting a series of roughly equally spaced peaks with mechanical admittance values of the same order.

To determine the location of the defect, the steady-state region between P_2 and P_4 was selected for the calculation, considering the peaks P_2, P_3, P_4 and P_5 to be similar and thus defining a periodic behaviour. From peaks P_2 and P_4 one can thus obtain

(1) $2\Delta f = f_{p4} - f_{p2} = 948{\cdot}7 - 329 = 619{\cdot}7$ 1/s (or Hz),
(2) $H_T + F_H = V_{rod}/2\Delta f = 3790/619{\cdot}7 = 6{\cdot}12$ m,
(3) error per cent $= (6{\cdot}12 - 6)/6 \times 100$ per cent $= 2$ per cent.

The theoretical distance between the top of the pile and the neck is $H_T + F_H = 1 + 5 = 6$ m. The error in the prediction is 2 per cent. A further examination indicates that P_9 and P_{17} can be selected as another periodic event since the curve in the range from P_8 to P_{10} is very similar to that from P_{16} to P_{18}. The associated information it represents is the length of the neck:

(1) $\Delta f = f_{p17} - f_{p9} = 3786 - 1904 = 1882$ Hz,
(2) $F_L = V_{rod}/2\Delta f = 3790/3764 = 1{\cdot}01$ m,
(3) error per cent = 1 per cent.

This observation will be verified later as the length of the neck is increased from 1 to 2 m.

3.1.2. Bulb. The pile with a bulb shown in Figure 1(b) with $F_H = 5$, $F_R = 0{\cdot}2$, and $F_L = 1$ m was studied next. The displacement time histories obtained with the 1-D and 3-D models are presented in Figure 5(a). The original and the filtered results from the 3-D models are compared in Figure 5(b). It should be noticed that in this case the filtering with a threshold frequency of 500 Hz was not as effective as in the previous one and some small fluctuations remained in the

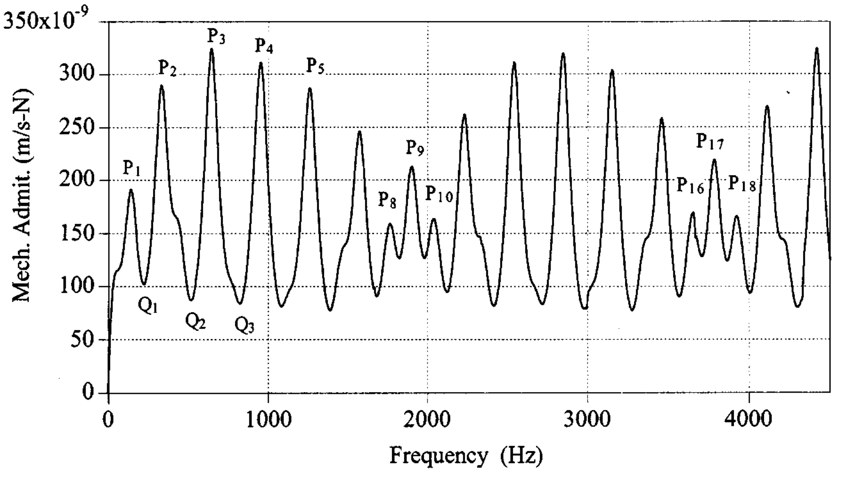

Figure 4. Mechanical admittance of a pile containing a neck with $F_H = 5$, $F_R = 0{\cdot}2$, and $F_L = 1$

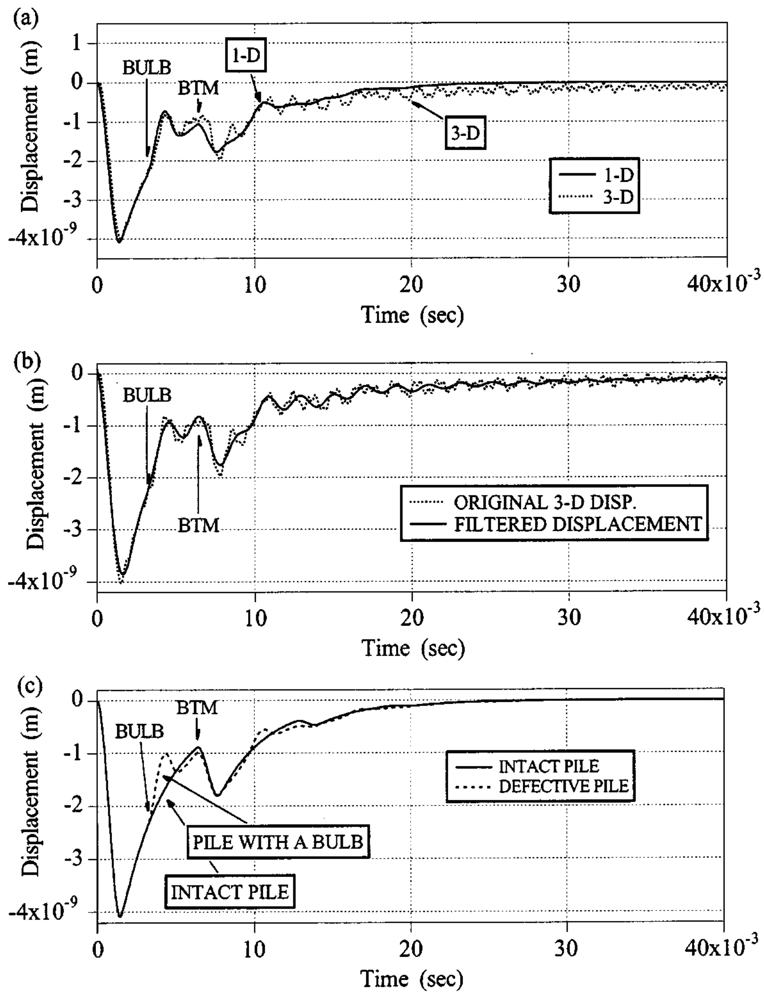

Figure 5. Displacement at top of a pile containing a bulb with $F_H = 5$, $F_R = 0{\cdot}2$, and $F_L = 1$, using (a) 1-D and 3-D models, (d) original and filtered 3-D results ($f_H = 500$ Hz) and (c) 1-D results in comparisons with those of an intact pile

record. The agreement with the 1-D solution is still very good. Shown in Figure 5(c) is the comparison between the 1-D results for an intact pile and a defective pile with a bulb. The theoretical times of arrival of the P-waves reflected from the neck and the bottom are marked in the figure with 'BULB' and 'BTM'.

It can be seen that a bulb results in a peak in the variation of the displacement (a reduction in its amplitude) instead of the dip (an increase in magnitude) that occurred in the case of a neck. It is also seen that identifying the existence and location of a bulb from the displacement response at the top of the pile may be harder than that of a neck (particularly if a solution for the intact pile as a benchmark is not available).

The associated velocity time histories are presented in Figure 6. It is seen that a bulb results in a clear bump (beginning at 'BULB') in the velocity records and thus using the velocity to locate a bulb is easier than using the displacement. It should also be noticed that the filtering for the velocity record with a threshold frequency of 1000 Hz is also less effective than for the pile with

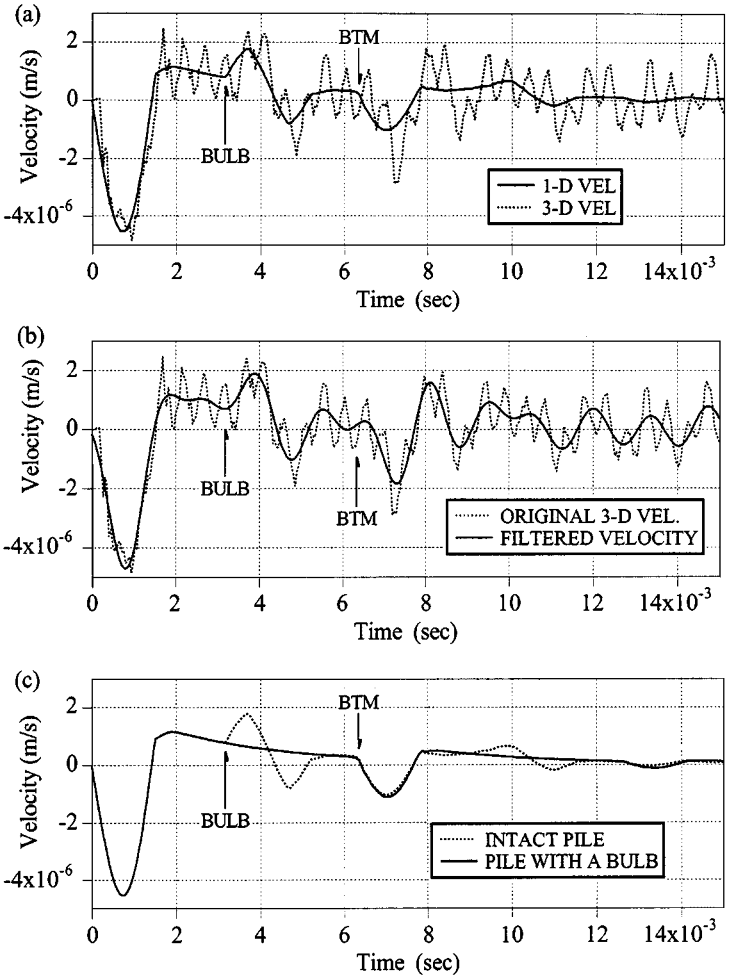

Figure 6. Velocity at top of a pile containing a bulb with $F_H = 5$, $F_R = 0{\cdot}2$, and $F_L = 1$, using (a) 1-D and 3-D models, (d) original and filtered 3-D results ($f_H = 500$ Hz) and (c) 1-D results in comparisons with those of an intact pile

a neck. The filtered 3-D solution is still in good agreement with the results of the 1-D model for times below 5×10^{-3} s (this is the most important time interval) but deteriorates later.

The corresponding mechanical admittance curve is presented in Figure 7. To locate the bulb, the peaks with an amplitude of the same order, P_4, P_6 and P_8 were selected for the calculation.

(1) $2\Delta f = f_{p8} - f_{p4} = 1102 - 488{\cdot}1 = 613{\cdot}9$ Hz,
(2) $H_T + F_H = V_{rod}/2\Delta f = 6{\cdot}17$ m.

The percentage error is only 2·8 per cent.

It is also seen that P_{13} and P_{25} can be selected as another periodic event and therefore their frequency difference was selected to estimate the length of the bulb:

(1) $\Delta f = f_{p25} - f_{p13} = 3786 - 1898 = 1888$ Hz,
(2) $F_L = V_{rod}/2\Delta f = 1{\cdot}00$ m,
(3) error per cent $= 0$.

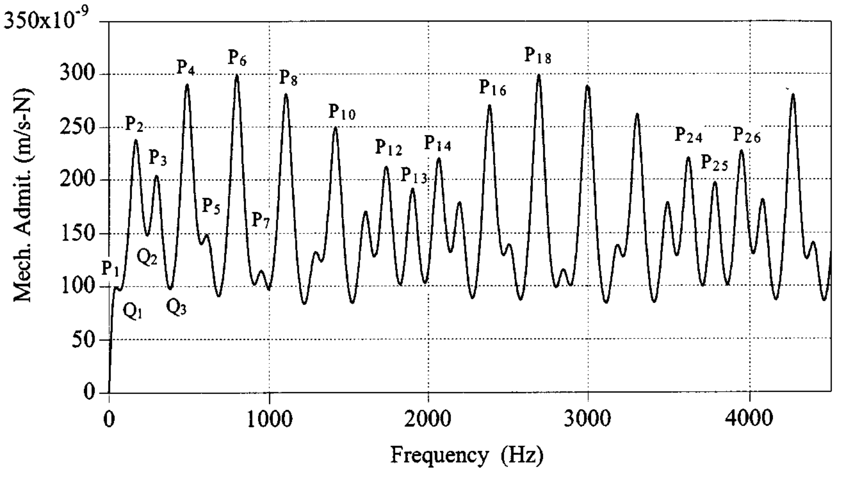

Figure 7. Mechanical admittance of a pile containing a bulb with $F_H = 5$, $F_R = 0{\cdot}2$, and $F_L = 1$

There is again no error in this estimation. A comparison of Figure 7 (for a bulb) with Figure 4 (for a neck) shows that the peak P_{13} for the mechanical admittance curve of the pile with a bulb has an amplitude smaller than the two neighbouring peaks (P_{12} and P_{14}) while the opposite is true for peaks P_9, P_8 and P_{10} in the case of a neck.

3.2. *Effect of length of defect*

3.2.1. Neck. The length of the neck discussed in Section 3.1.1 was increased from $F_L = 1$ to $F_L = 2$ m. The displacement time histories obtained from the 1-D and the 3-D models are shown in Figure 8(a) and 8(b), respectively, in conjunction with the results obtained in Section 3.1.1 where $F_L = 1$ m. It can be seen that an increase in the length of the neck results in an increase in the amplitudes of the dip associated with 'NECK'. However, the differences are so small that characterizing the length of the neck from the time-domain solutions is very difficult. This situation can be much improved as the mechanical admittance analysis is carried out. It is also seen that the times of arrival of the waves are not affected by changing the length of the neck, but depend only on the depth at which the neck starts.

The velocities corresponding to the displacements shown in Figure 8(a) are presented in Figure 8(c). It is seen that using the time-domain solution to determine the existence and location of the neck is much easier than to determine its length.

The mechanical admittance curve is shown in Figure 9. The neck can be located using the periodic events corresponding to P_2 and P_3:

(1) $\Delta f = f_{p3} - f_{p2} = 625{\cdot}2 - 329 = 296{\cdot}2$ Hz,
(2) $H_T + F_H = 6{\cdot}40$ m,
(3) error per cent = 6·7 per cent.

It is seen that the shape of the curve between peaks P_{11} and P_{13} is very similar to that observed in Figure 4 between P_8 and P_{10}. However in this case, similar events also occur around P_5 and P_{18}.

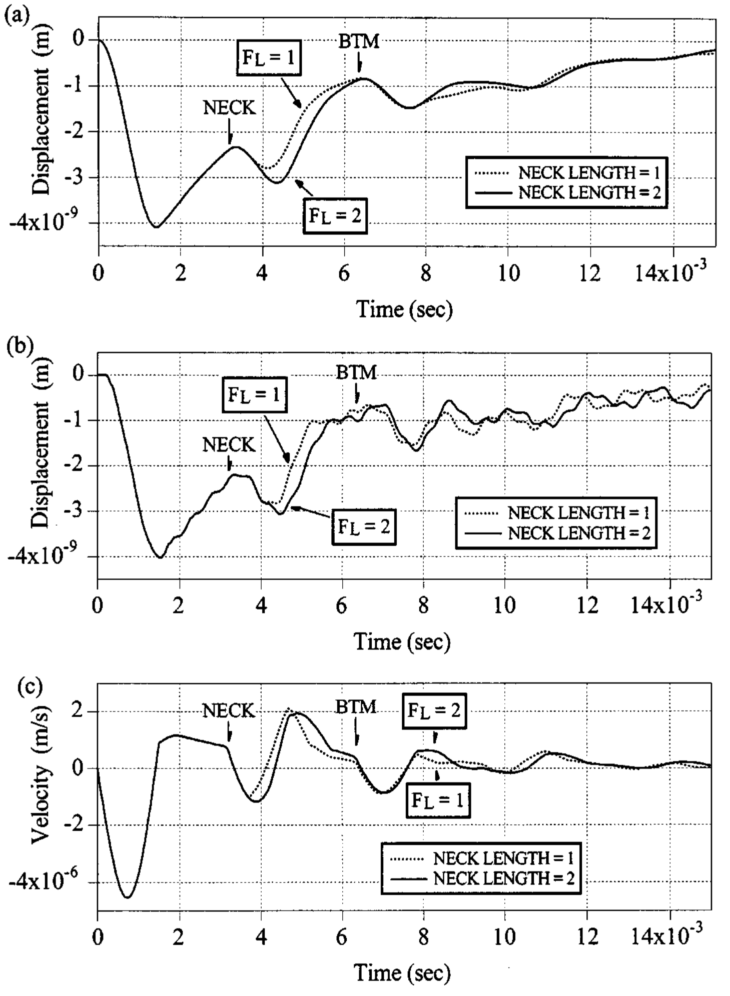

Figure 8. (a) 1-D, (b) 3-D displacement, and (c) 1-D velocity at top of a pile containing a neck with $F_H = 5$, $F_R = 0{\cdot}2$, $F_L = 1$ and 2

The periodic events corresponding to P_5, P_{12} and P_{18} can thus be used to determine the length of the neck:

(1) $2\Delta f = f_{p18} - f_{p5} = 2824 - 948{\cdot}7 = 1875{\cdot}3$ Hz,
(2) $F_L = 2{\cdot}02$ m,
(3) error per cent $= 1{\cdot}1$ per cent.

3.2.2. Bulb. A bulb with different lengths $F_L = 1$ and $F_L = 2$ m was then considered. The displacements for piles with these bulbs are shown in Figures 10(a) and 10(b) for the 1-D and the 3-D results. It can be seen that an increase in the length of the bulb increases the amplitude of the peak in the displacement curve beginning at 'BULB'. The velocities corresponding to the displacements shown in Figure 10 are presented in Figure 10(c). Observations similar to those made previously for necks and for the 1 m bulb apply to these results.

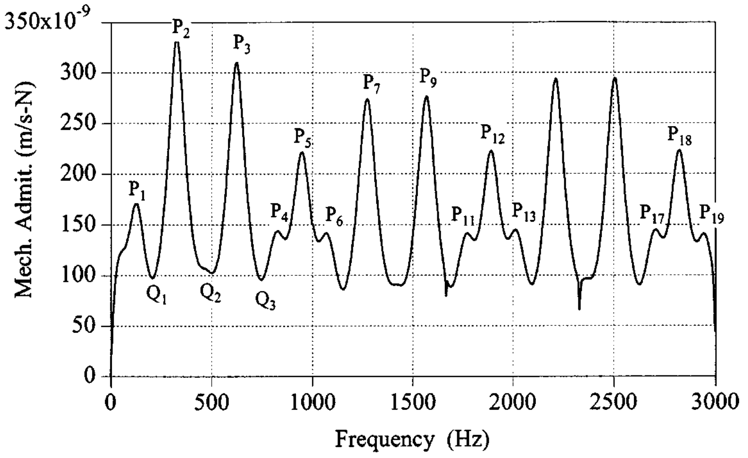

Figure 9. Mechanical admittance of a pile containing a neck with $F_H = 5$, $F_R = 0{\cdot}2$, and $F_L = 2$

The mechanical admittance curve for $F_L = 2$ m is shown in Figure 11. The location of the bulb can be determined using the periodic events corresponding to P_2, P_4 and P_6:

(1) $2\Delta f = f_{p6} - f_{p2} = 608{\cdot}7$ Hz,
(2) $H_T + F_H = 6{\cdot}23$ m,
(3) error per cent = 3·8 per cent.

To estimate the length of the bulb, the periodic events associated with P_7, P_{14} and P_{21} are selected.

(1) $2\Delta f = f_{p21} - f_{p7} = 1875{\cdot}3$ Hz,
(2) $F_L = 2{\cdot}02$ m,
(3) error per cent = 1·1 per cent.

Once again the shapes for the periodic events around P_7 (or P_{14}) are the opposite of those around P_5 (or P_{12}) for the pile with a neck.

3.3. Effect of width of defect

3.3.1. Neck. The width of the neck discussed in Section 3.1.1 was increased from $F_R = 0{\cdot}2$ to $F_R = 0{\cdot}4$ m. The displacements for $F_R = 0{\cdot}2$ and 0·4 m are shown in Figures 12(a) and 12(b) for the 1-D and the 3-D results. It is seen that the increase in the width of the neck results in a very pronounced increase in the amplitude of the downward displacement. As the width of the neck increases, the stiffness of the pile in the defective zone decreases, resulting in an increased displacement. This is qualitatively similar to what was observed when the length of the neck was increased. The velocities corresponding to the displacements of Figure 12(a) are shown in Figure 12(c).

The mechanical admittance curve corresponding to $F_R = 0{\cdot}4$ m is presented in Figure 13. Using any two peaks such as f_{p2} and f_{p4} the depth at which the neck starts is calculated to be 6·07 m. The error is only 1·1 per cent. Although the picture is less clear, P_8 can still be selected to

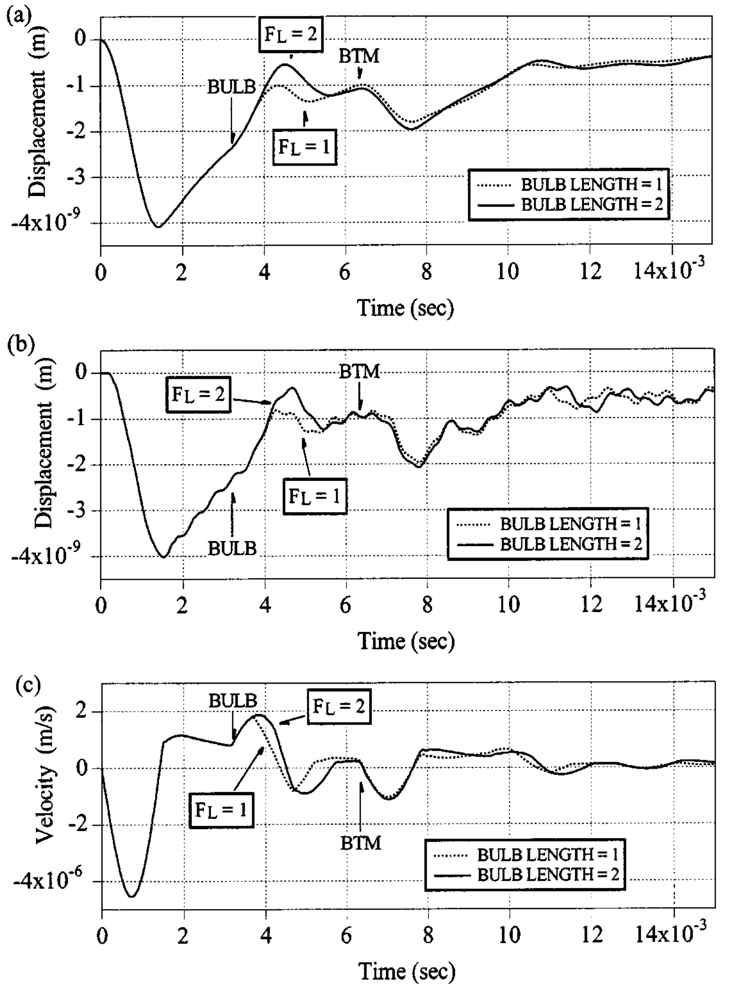

Figure 10. (a) 1-D, (b) 3-D displacement, and (c) 1-D velocity at top of a pile containing a bulb with $F_H = 5$, $F_R = 0{\cdot}2$, $F_L = 1$ and 2

calculate the length of the neck since it is the lowest peak in the steady-state region. Using $f_{p8} = 1892$ Hz the length of the neck is again determined to be 1 m. The error in predicting the length of the neck in this case is again zero.

3.3.2. Bulb. The width of the bulb discussed in Section 3.1.2 was increased from 0·2 to 0·4 m. The displacements for $F_R = 0{\cdot}2$ and $F_R = 0{\cdot}4$ m are shown in Figures 14(a) and 14(b) for the 1-D and the 3-D results, respectively. As in previous cases the existence of a bulb results in a bump (rather than a dip) in the displacement with the amplitude of the displacement decreasing. This bump is more pronounced as the width of the bulb increases. The velocities corresponding to the displacements of Figure 14(a) are shown in Figure 14(c).

The mechanical admittance function presented in Figure 15 corresponds to the case when the width of the bulb is 0·4 m. P_4, P_5, P_6 and P_7 were selected to assess the location of the bulb.

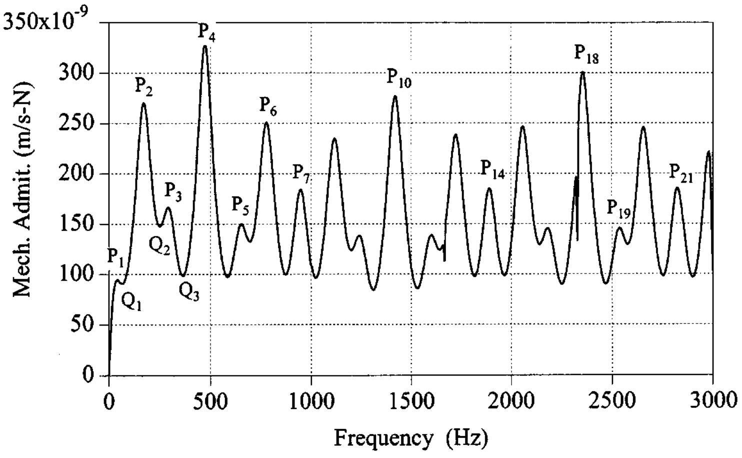

Figure 11. Mechanical admittance of a pile containing a bulb with $F_H = 5$, $F_R = 0{\cdot}2$, and $F_L = 2$

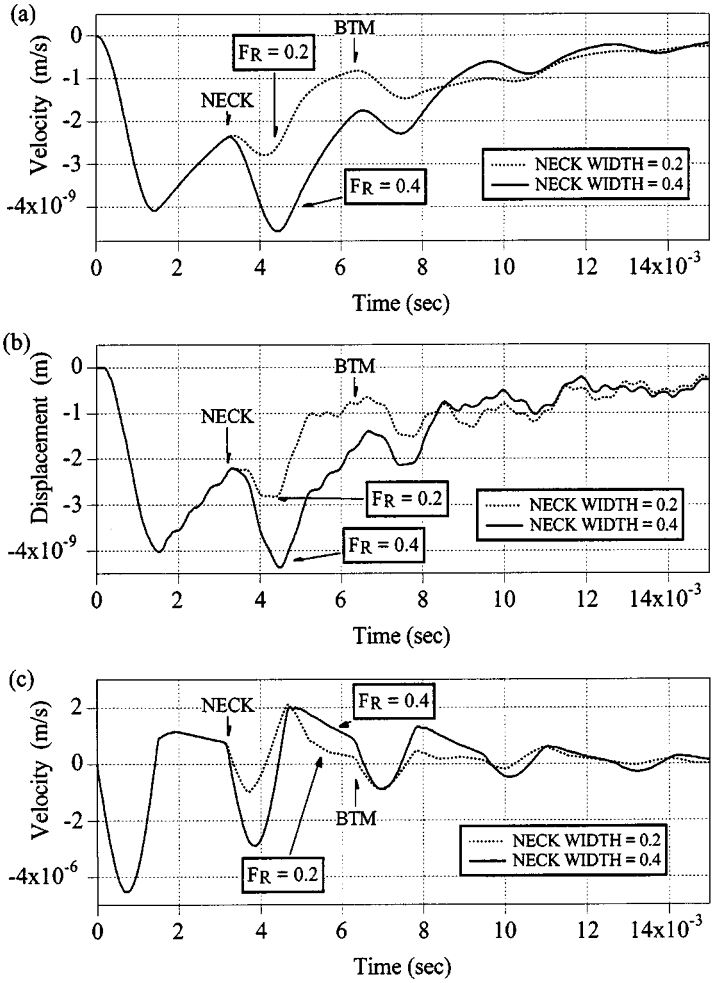

Figure 12. (a) 1-D, (b) 3-D displacement, and (c) 1-D velocity at top of a pile containing a neck with $F_L = 1$, $F_H = 5$, $F_R = 0{\cdot}2$ and $0{\cdot}4$

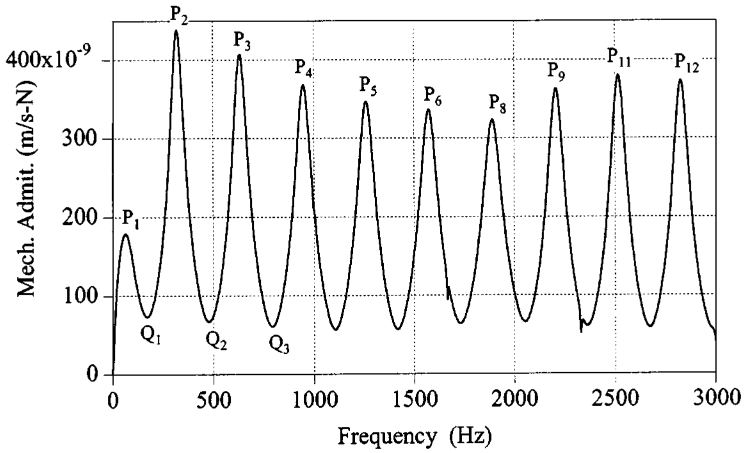

Figure 13. Mechanical admittance of a pile containing a neck with $F_H = 5$, $F_R = 0{\cdot}4$, and $F_L = 1$

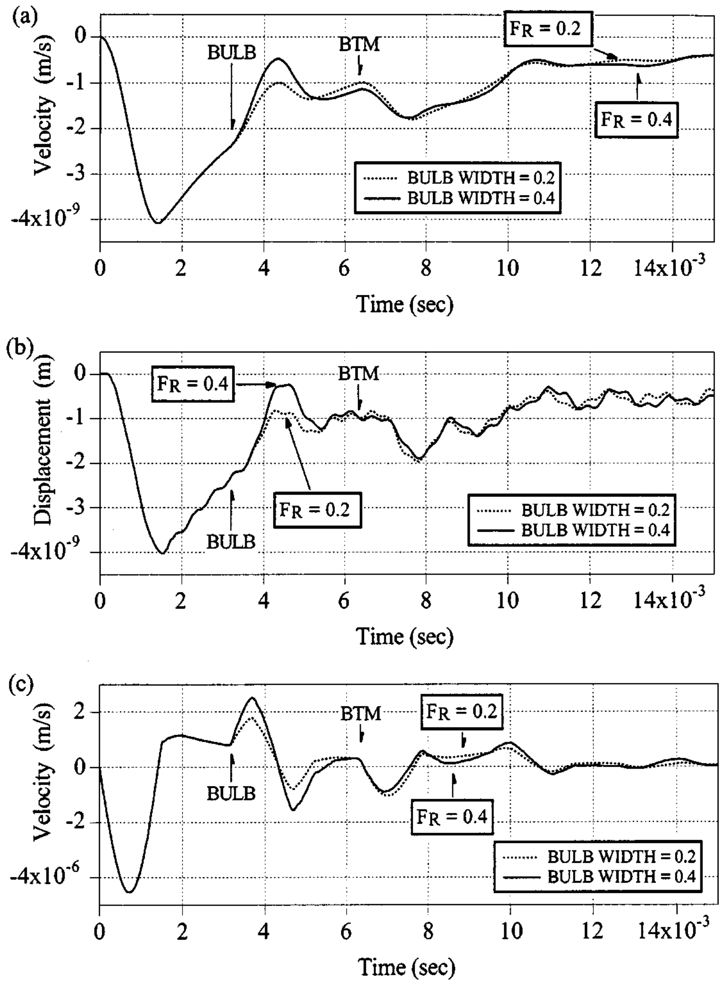

Figure 14. (a) 1-D, (b) 3-D displacement, and (c) 1-D velocity at top of a pile containing a bulb with $F_L = 1$, $F_H = 5$, $F_R = 0{\cdot}2$ and $0{\cdot}4$

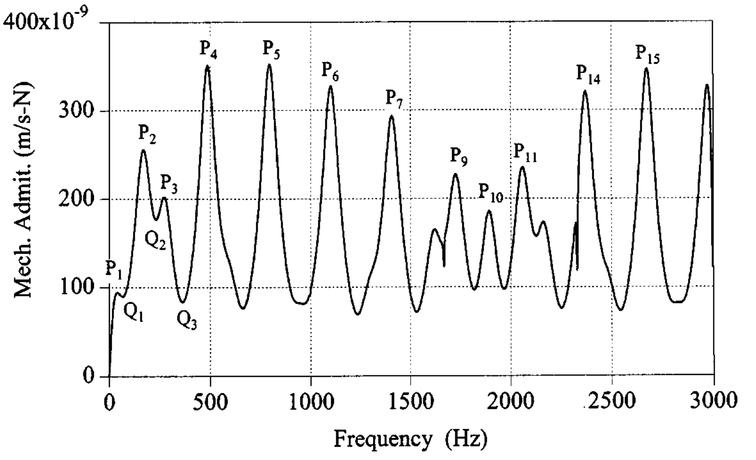

Figure 15. Mechanical admittance of a pile containing a bulb with $F_{\mathrm{H}} = 5$, $F_{\mathrm{R}} = 0{\cdot}4$, and $F_{\mathrm{L}} = 1$

(1) $3\Delta f = f_{p7} - f_{p4} = 920{\cdot}9$ Hz,
(2) $H_{\mathrm{T}} + F_{\mathrm{H}} = V_{\mathrm{rod}}/2\Delta f = 6{\cdot}17$ m,
(3) error per cent = 2·8 per cent

The symmetric point of the figure is P_{10} and therefore the length of the bulb was calculated to be $F_{\mathrm{L}} = 1$ m with excellent accuracy. Comparison of the results shown in Figure 13 for a neck and Figure 15 for a bulb indicates that the shape of the mechanical admittance function remains essentially unchanged as the width of the bulb increases and thus the determination of the length of the defect is not affected. On the other hand when the width of the neck is reduced and becomes very small the determination of the length becomes increasingly difficult, as could be expected.

4. CONCLUSION

The results of the studies conducted indicate that the mechanical admittance function can provide very reasonable estimates not only of the location but also the length of an axisymmetric neck or a bulb in a pile. In both the time and frequency domain records, a neck can be detected and distinguished from a bulb. However, locating a neck would appear to be easier than a bulb. The depth of a defective zone can be obtained with good accuracy. From the cases examined in this work, the determination of the length of a defective zone is only possible in the frequency domain. Identifying multiple defective zones at different depths (a topic not covered in this paper) is still difficult.[2] In the case of intact piles there is a limitation in the total length of the pile for which the reflections from the bottom can be identified in the records obtained at the top. Obviously this limitation would also apply to the depth at which defects can be located.

The interpretation of the data collected in this type of tests is normally carried out using one-dimensional model. The actual data should be closer, however, to the predictions of the 3-D models and therefore somewhat less clear. The use of filters to eliminate high-frequency terms is therefore recommended. With these filters the 3-D effects can be minimized.

REFERENCES

1. S. T. Liao and J. M. Roesset, 'Dynamic response of intact piles to impulse loads', submitted to *Int. J. Numer. Anal. Methods Geomech.*, **21,** 255–275 (1997).
2. S. T. Liao, 'Nondestructive testing of piles', *Ph.D. Dissertation*, University of Texas at Austin, 1994.